

Coronal quasi-periodic fast-propagating magnetosonic waves observed by SDO/AIA

Yuandeng Shen

Yunnan Observatories, Chinese Academy of Sciences, Kunming 650216, China
email: ydshen@ynao.ac.cn

Abstract. Coronal quasi-periodic fast-propagating (QFP) magnetosonic waves are scarce in previous studies due to the relative low temporal and spatial resolution of past telescopes. Recently, they are detected by the Atmospheric Imaging Assembly (AIA) on board the Solar Dynamics Observatory (SDO). Here, two cases of QFP waves are presented. The analysis results indicate that QFP waves are tightly associated with the associated flares. It is indicated that QFP waves and the associated flares are possibly driven by the same physical process such as quasi-periodic magnetic reconnection process in producing flares.

Keywords. Waves, Flares, Magnetic fields, Oscillations, Atmosphere

1. Introduction

The observations of coronal QFP waves are usually imaged by the SDO/AIA 171 Å channel. They are always associated with flares, and have multiple arc-shaped wavefronts that emanate successively from the flare kernel and propagate outward along coronal loops. Their speed can range from several hundred to a few thousand km s^{-1} , and the periods are of tens of seconds to a few minutes. The first QFP wave was reported by Liu *et al.* 2011. From then on, the QFP wave has attracted a lot of attention due to the possible application in coronal seismology and the role played in the coronal heating problem. So far, more observations have been documented in (e.g., Shen & Liu 2012, Liu *et al.* 2012, Shen *et al.* 2013, Yuan *et al.* 2013, Nisticò *et al.* 2014, Kumar & Innes 2015). In the meantime, simulation experiments have also been performed to understand the driving mechanism and propagation properties of QFP waves (Ofman *et al.* 2011, Pascoe *et al.*, 2013, 2014, Yang *et al.* 2015). Here, two QFP wave events are analyzed to provide some new clues for understanding the driven mechanism and propagation properties of QFP waves.

2. Results

The first QFP wave case occurred on May 30, 2011, which accompanied by a C2.8 flare and imaged by the SDO/AIA 171 Å channel. The wave trains emanated from the flare kernel successively and propagated along a group of open coronal loop, and the wavefronts could be divided into three sub QFP waves (see arrows in Figure 1. (b)–(c)), which have different periods, amplitude, and phase speeds, but they are all related to impulsive radio bursts (Yuan *et al.* 2013). A k – ω diagram is generated over the wavefront region, which reveals that there are many frequencies in the wave (see Figure 1. (e)). By analyzing the frequencies of the associated flare, it is found that the flare's frequencies are all included in the QFP wave's frequency spectrum. This suggests that the flare and the QFP waves were possibly excited by a common physical process. On the other hand, a few low frequencies (e.g., 2.5 and 0.7 mHz) revealed by the k – ω diagram cannot be found in the accompanying flare. This is possibly due to the leakage of the pressure-driven oscillations from the photosphere into the low corona, which should be a noticeable

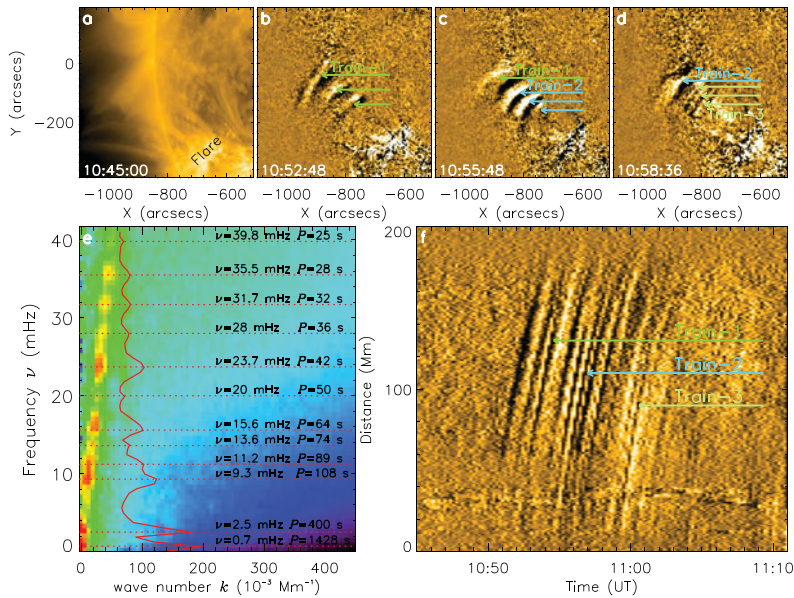


Figure 1. The QFP wave on May 30, 2011. a, direct 171 Å image. b – d, running difference 171 Å images with arrows indicating the wave trains. e, Fourier power (k – ω) of the 171 Å running difference images during 10:48–11:00 UT over the wavefront region. f, time-distance plot obtained from 171 Å running difference images along a line perpendicular to the wavefronts, and arrows indicating the propagating wave trains.

mechanism for driving QFP waves in corona. The time-distance plot shows that the phase speeds of three sub QFP waves are 735, 845, and 820 km s^{−1}, and their decelerations are 1.35, 2.27, and 1.31 km s^{−2}, respectively.

The other QFP wave occurred on April 23, 2012, which accompanied by a C2.0 flare and propagated along a loop system (see Figure 2. (a)–(c)). A flare ribbon near the guiding loop’s footpoint may directly lead to the QFP wave. The wave trains are firstly observed in AIA 171 Å images, after the interaction with a perpendicular loops on the path, they suddenly appeared in the 193 Å channel (see Figure 2. d–e). The average phase speeds before and after the interaction are about 689 and 343 km s^{−1} in the 171 Å, and it is about 362 km s^{−1} in the 193 Å. Periodic analysis indicate that the periods of the QFP wave before and after the interaction are all of 80 s in the 171 Å observations, and that measured from the 193 Å images are also the same. Interestingly, the period of the accompanying flare is the same with the wave trains, suggesting that the QFP wave and the flare are all the result of a common physical process.

3. Conclusions and Discussions

Based on the two cases of QFP waves, one main common characteristic is that QFP waves have similar periods with the associated flares. This indicate that QFP waves and flares are the two sides of manifestations of a single physical process. Analysis results indicate that the periodic releasing of energy bursts through some nonlinear processes in the magnetic reconnection process, which produces flares, could be a possible explanation.

In the second event, the sudden deceleration of the wave trains in 171 Å images and their appearance in 193 Å observations could be interpreted through a geometric effect and the density increase of the guiding loop system, respectively. It is well known that the distribution of magnetic fields is very complex, but the basic configuration should

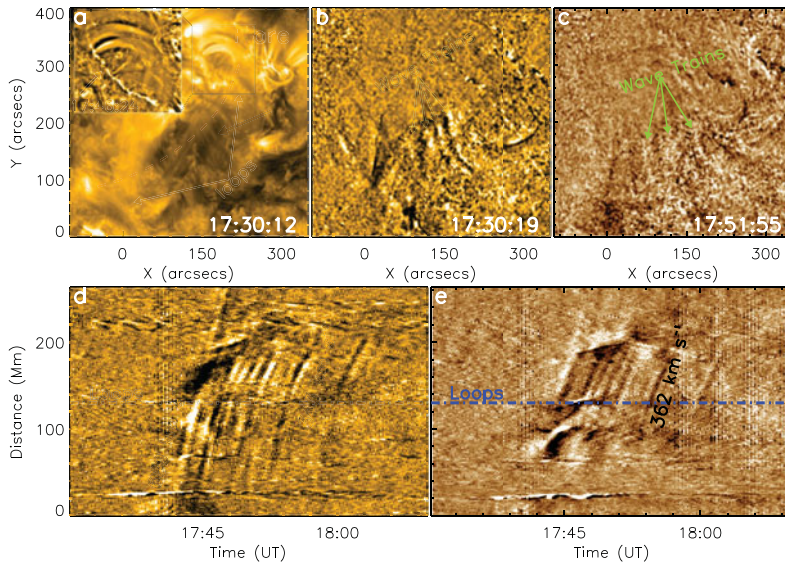


Figure 2. The QFP wave on April 23, 2012. a, direct 171 Å image. b and c, 171 Å and 193 Å running difference images, respectively. d and e, time-distance plots made from 171 Å and 193 Å running difference images along the dashed curve showing in panel a. The inset in panel a shows the detail of the flare region, and the blue dashed lines in panels d and e indicate the position of the perpendicular loop.

be an upward funnel-like shape. Here, the guiding loops may change their inclination angle significantly when approaching the perpendicular loop system, and thus become more curved upwardly. Therefore, due to the projection effect the observed wave speed can decrease to a small value within a short timescale. On the other hand, when the wave-guiding loops interact with the perpendicular loops, the wave trains will cause a strong compression of the guiding fields, which would increase the density of the guiding loops quickly and thereby decrease the speed of the wave trains within a short timescale. In addition, the compression can still cause a possible adiabatic heating that dissipates the wave energy and thus result in the wave trains in the 193 Å observations.

Acknowledgements

This work is supported by Chinese foundations (11403097, 2015FB191), and the Youth Innovation Promotion Association (2014047).

References

- Kumar, P. & Innes, D. E. 2015, *ApJ*, 803, 23
 Liu, W., Title, A. M., Zhao, J. W., Ofman, L., & Schrijver, C. J., *et al.* 2011, *ApJL*, 736, L13
 Liu, W., Ofman, L., Nitta, N. V., Aschwanden, M. J., & Schrijver, C. J., *et al.* 2012, *ApJ*, 753, 52
 Nisticò, G., Pascoe, D. J., & Nakariakov, V. M. 2014, *A&A*, 569, A12
 Ofman, L., Liu, W., Title, A., & Aschwanden, M. 2011, *ApJL*, 740, 33
 Pascoe, D. J., Nakariakov, V. M., & Kupriyanova, E. G. 2013, *A&A*, 560, 97
 Pascoe, D. J., Nakariakov, V. M., & Kupriyanova, E. G. 2014, *A&A*, 568, A20
 Shen, Y. & Liu, Y. 2012, *ApJ*, 753, 53
 Shen, Y., Liu, Y., Su, J. T., Li, H., & Zhang, X. F., *et al.* 2013, *SoPh*, 288, 585
 Yang, L., Zhang, L., He, J., Peter, H., Tu, C., *et al.* 2015, *ApJ*, 800, 111
 Yuan, D., Shen, Y., Liu, Y., Nakariakov, V. M., & Tan, B., *et al.* 2013, *A&A*, 554, A144